Journal of Oceanography and Marine Science Vol. 3(3), pp. 41-55, December, 2012
Available online http://www.academicjournals.org/joms
DOI: 10.5897/JOMS12.001
ISSN 2141-2294 ©2012 Academic Journals

Full Length Research Paper

Radiological and mineralogical investigation of accretion and erosion coastal sediments in Nile Delta Region, Egypt

Ayman A. El-Gamal[1]* and Ibrahim H. Saleh[2]

[1]Marine Geology Department, Coastal Research Institute, National Water Research Center, 15, St. Elpharanaa, Elshalalat, Postal Code 21514, Alexandria, Egypt.
[2]Environmental Studies Department, Institute of Graduate Studies and Research, Alexandria University, P. O. Box 832, El-Shatby, Alexandria, Egypt.

Accepted 8 February, 2012

The Nile Delta coast is a dynamic sedimentary environment experiencing erosion, transport and re-deposition of sand along the coast. The aim of this study was to investigate the effectiveness of using an integrated approach of natural radioactivity of coastal sediments, heavy mineral distribution and grain size information to differentiate between the eroding and accreting areas of the Nile Delta coast. Also, it is to investigate the relationship between grain size and heavy mineral distributions of these sediments on the spatial distribution of the coastal radioactive materials. The relatively higher profile averages of ^{226}Ra, ^{214}Pb, ^{214}Bi and ^{210}Pb (as ^{238}U series) were 104.37±84.66, 45.60±37.83, 38.43±32.49 and 35.69±24.86 Bq/kg, respectively and ^{228}Ra and ^{212}Pb (as ^{232}Th series) were 54.26±56.66 and 42.18±44.66 Bq/kg, respectively. The highest average value of ^{40}K concentration (404.49±125.81 Bq/kg) was detected in the profile located at 2000.1 m west of Rashid estuary. Microscopic study revealed that the more dominant heavy minerals assemblages consisted of Opaques, Hornblende, Augite, Epidote, Biotite and Chlorite. Also, minor amounts of Garnet, Zircon, Rutile, Tourmaline, Kyanite and Monazite have been identified. Relatively high concentrations of ^{238}U and ^{232}Th series members were found in coincident at sites having higher heavy minerals percentages and detected at erosional beach than the accretion one. Coincidence was recognized between the average concentrations of ^{40}K and the percentages of the light minerals collected at 100 m distances of the profiles under investigation.

Key words: Nile Delta, beach erosion, beach accretion, natural radioactivity, heavy minerals.

INTRODUCTION

Coasts are dynamic systems, undergoing adjustments of form and process at different time and space scales in response to geomorphological and oceanographical factors (Cowell et al., 2003). Beach sands are mineral deposits formed through erosion of geological formations which may have been brought to their present location after transport by wind, rivers and glaciers to the coast, and are deposited on the beaches by actions of waves and currents (de Meijera et al., 2001). Nile River is the main source of the Nile Delta beach sands. In the past, Nile River transported black sand from mountain ranges of Sudan and Abyssinia to its delta in the Mediterranean coast of Egypt. This black sand contains anomalies of relatively higher natural radioactive nuclides than the other coastal sands (El-Naggar, 1990; El-Khatib et al., 1993; El-Gamal et al., 2004; Hussein, 2011). This sedimentation was cut off after building of Aswan High Dam.

*Correspondence author. E-mail: ayman_elgamal@yahoo.com.

The principal primordial radionuclides are isotopes of heavy elements (USEPA, 2011). Natural radioactivity in sediments comes from uranium (^{238}U) and thorium (^{232}Th) series and natural potassium (^{40}K) (Veigaa et al., 2006) which are detected in the Egyptian Mediterranean coastal sediments (El-Gamal et al., 2004; Saleh et al., 2004). Traces of artificial radionuclides such as cesium (^{137}Cs) can also be present, as a result of the fallout from weapons testing and from Chernobyl accident (Johanson and Bergström, 1989). The variability in ^{238}U and ^{232}Th series across the shore profiles is mainly explained by variations in heavy and light mineral contents. Typically, higher percentages of heavy minerals will result in higher concentrations of primordial radionuclides (Brai et al., 2006). Such variability can be accounted by redistribution of the sand caused by erosion/deposition processes. Furthermore, parameters such as grain size and heavy minerals content were studied in connection with the distribution of U, Th and ^{40}K by de Meijer (1998), Seddeek et al. (2005) and Vassas et al. (2006). Therefore the enriched areas with U and Th, presumably result from the sorting of sand grains according to their size and density (Vassas et al., 2006).

In the Nile Delta, Egypt, the distribution of heavy mineral assemblages has been recognized as two mineral groups (Frihy et al., 1995; Frihy, 2007). The first group includes heavy minerals of lower density and coarser size (augite, hornblende and epidote). Heavy minerals in this group increase from west to east along the delta as they are easily to entrain and transport the coastal sediments toward the east by wave currents. In contrast, the second group includes heavy minerals of higher-density (opaques, garnet, zircon, rutile, tourmaline and monazite) and these minerals are difficult to entrain and transport by wave-current actions. Hence, minerals in this group form a lag deposit within the delta and beach sand.

De Meijer et al. (1990) and de Meijer and Donoghue (1995) concluded that the origin (provenance) of beach sands can be estimated from the radiometric fingerprints of its light and heavy minerals. The radiometric fingerprint is a set of activity concentrations of ^{40}K, ^{232}Th and ^{238}U (de Meijer, 1998). The heavy minerals such as monazite contain overall an order of magnitude less ^{40}K and two orders of magnitude more of ^{232}Th and ^{238}U, compared to light minerals. Radiometric analysis of various fractions of heavy mineral sands showed that the monazite and zircon sands are highly radioactive contents (U and Th) as compared to other minerals in the heavy mineral suite (Alam et al., 1999; Mohanty et al., 2004; Coelho et al., 2005). The abundance of thorium typically about 10 wt% and that of U about 0.5 wt% are found in monazite crystals. Zircon typically contains 5 to 4000 ppm of U and 2 to 2000 ppm of Th (Deer et al., 1997; Mohanty et al.; 2004). On the other hand, chlorite, biotite, tourmaline, apatite, magnetite and quartz may contain uranium (Dahlkamp, 2009).

Heavy mineral grains are generally more difficult to entrain and transport by currents than other light mineral grains of the same shape and size, and thus, heavy minerals are represented by smaller grains (Kudrass, 1987; Komar, 2007). However, heavy minerals grains with lower mobility values such as zircon, tourmaline, coarse garnet and staurolite tend to remain relatively close to their input sources and thus these minerals are common in the inner-shelf zones near estuaries (Cascalho and Fradique, 2007). The deposition of materials such as heavy minerals requires a high-energy level, which can occur during storm episodes. This may explain why heavy minerals are mainly observed on erosion beaches where the shoreline has retreated, as observed along the Nile Delta (Frihy et al., 1995). High-density materials tend to become concentrated in areas of beach erosion, accounting for the formation of enriched radioactive sand, whereas minerals of lower density and coarse size are selectively entrained by waves and current and preferentially transported to zone of beach accretion where they are deposited (Frihy and Komar, 1993; Frihy et al., 1995). Such a process is widely supported by the inverse correlation observed in sand samples between ^{40}K that is a tracer of light minerals (Seddeek et al., 2005; de Meijer, 1998). These previous studies suggested an inverse correlation between grain size and radioactivity with the finest fraction being enriched by about three orders of magnitude (de Meijer, 1998). Uranium and thorium isotopes have been used commonly as radiotracers for studies of marine sediments, including their sources, transport and sedimentation rates in relation to the sedimentary and geochemical processes in the marine environment (Cochran and Krishnaswami, 1980; Li et al., 1985; Cole et al., 1986; Suman and Bacon, 1989).

The aim of this study was to investigate the effectiveness of using an integrated approach of natural radioactivity of coastal sediments, heavy mineral distribution and grain size information to differentiate between the eroding and accreting areas of the Nile Delta coast. The study of the distribution of primordial radionuclides allows good understanding of the radiological implication of these elements due to coastal processing. The study also aimed to investigate the effects of grain size and heavy mineral distributions in sand on the spatial distribution of coastal radioactivity.

MATERIALS AND METHODS

Study area

During the past century, the Nile Delta was suffering from sever erosion and vast retreating in shoreline especially at Rosetta, El-Burullus and Damietta headlands. So, many protection works have been executed along the Nile Delta coast to protect the eroded areas such as seawalls (for example, El-Burullus headland and the two sides of Rosetta Branch), detached breakwaters (for example, Baltim), groins (for example, eastern side of Rosetta) and jetties like

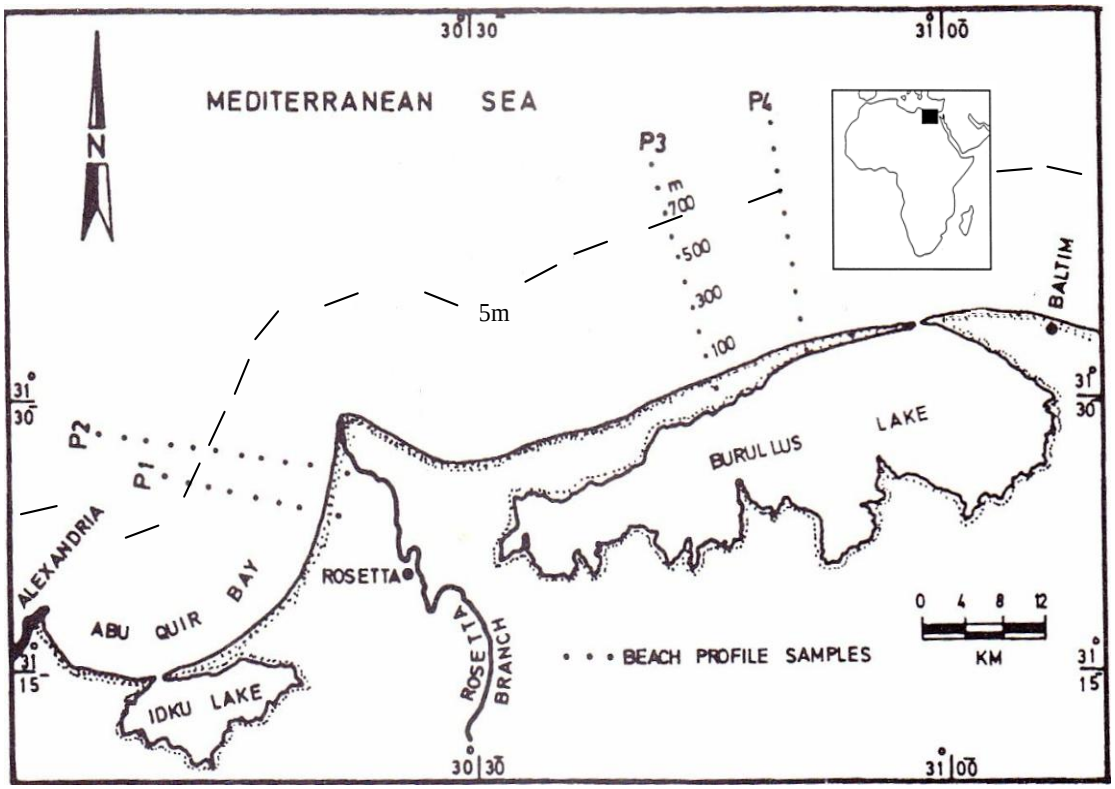

Figure 1. Sampling sites at Nile Delta area.

(for example, El-Burullus outlet) (CoRI, 2002). The hard structures attempt to change the regime of erosion and accretion at the beach. New sites are suffering by erosion while other sites gain more sediments than before the established of these protection tools.

Rashid promontory profiles

Rashid (Rosetta) promontory is located at the western mouth of the Nile River opening into the Mediterranean Sea (Figure 1). The western bank of Rashid was eroded with an average of −4 m/yr between 1978 and 1984 (Smith and Abdel-Kader, 1988). Coastal erosion and land retreat have persisted after the construction of the Rashid seawall (Nafaa, 1995). Downdrift erosion was generated when the seawalls became effective (Kaiser, 2004). Beach profiles have a steep face with no berm and many deep and wide bars and troughs. Many bars and troughs were observed at 25 to 250 m distance offshore at 1 to 5 m water depth. Storm waves destroy the berm as a result of a high intensity wave swash, and sediment was shifted offshore to form one or more bars that extend parallel to the shoreline (Miller, 1976). Beach profile configuration does not change significantly beyond 300 m seaward. The beach face (the seaward section of a beach exposed to and shaped by the action of waves) showed deposited sediment extending 150 m seaward and 2.5 m water depth (Kaiser and Frihy, 2009).

El-Burullus profiles

El-Burullus area is located between Rashid and Damietta promontories (Figure 1). Erosion has caused huge damage to the coastal regions at El-Burullus coastal area (El-Kolfat, 2005). The area west of El-Burullus has experienced continued accretion with rate of 4.9 m/yr due to the high rate of westward drift since the construction of the western jetty in 1972 (Badr and Lotfy, 1999; Frihy and Dewidar, 2003). The measured beach profiles showed a wide berm extending 200 m offshore with wide and shallow troughs and bars at 500 to 700 distance offshore and 5 to 6 m water depth. Beach profile morphology does not change significantly at distances more than 800 m offshore. It moved smoothly with a gentle slope (Kaiser and Frihy, 2009). The high concentrations of the heavy minerals at Rashid and El-Burullus sediments may be related to: 1. Contribution from offshore old sediments of classic Nile branches rather than the present Nile, 2. Contribution from the land itself, where the dunes and backshore contain great amount of these minerals and 3. These minerals are concentrated during severe coastal erosion (El-Fishawi and Badr, 1991).

Sampling

In October 2002 sediment sampling was carried out on west of Rashid (Rosetta) and El-Burullus beaches by Coastal Research Institute (CoRI) team using grab sampler from rubber boat (Zodiac). The marine survey has been carried out using geographical positioning system (GPS) and eco-sounder. A total of 36 surficial (0 to 15 cm depth) sediment samples were collected from 4 profiles (P1 to P4, position in Figure 1). Profiles P1 (31° 26.086' N and 30° 21.219' E) and P2 (31° 27.055' N and 30° 21.572' E) situated at 3892.6 and 2000.1 m distances west of Rashid Estuary, respectively representing the erosion coast. While profiles P3 (31° 33.438' N and 30° 52.946' E) and P4 (31° 34.165' N and 30° 55.524' E) located at 8917.4 and 4621.5 m distances west of El-Burullus Lake outlet, respectively representing the accretion coast. Beach profile lines are perpendicular to the coastline and extend from a fixed baseline in concrete blocks at the beach to 800 m

Table 1. Minimum detectable activities (MDAs) of the measured radionuclides.

Radionuclide	MDA (Bq/kg)
Cs-137	0.004
Pb-210	0.008
K-40	0.259
Pb-214	0.041
Bi-214	0.031
Ra-226	0.224

distances to about 6 m water depth by means of 100 m intervals (CoRI, 2002).

Radioactivity measurements

The dried samples were transferred to polyethylene containers of 100 cm^3. The radioactivity measurements were carried out using well-calibrated gamma spectrometry based on hyper-pure germanium (HPGe) detector, reverse electrode closed- end coaxial and extended range (Canberra Company). The 68 mm diameter and 69 mm length HPGe detector had a relative efficiency of 60%, and its resolution was 2.2 keV at 1.33 MeV, Peak/Compton effect was 60:1. The gamma transmissions used for activity calculations were 46.5 keV (^{210}Pb), 352.9 keV (^{214}Pb), 609.3, 1120.3 and 1764.5 keV (^{214}Bi), and 186 keV (^{226}Ra) for ^{238}U series, 338.4, 911.1 and 968.9 keV (^{228}Ac) for ^{232}Th series, 1460.7 keV for ^{40}K and 661.6 keV for ^{137}Cs. The calibration was carried out using standard sources. The quality control was carried out by parallel measurements of reference samples accumulated in containers with the same geometry and under the same measuring conditions and texture as for the actual samples. The reference materials were supplied by US DOE from mixed-analyte performance evaluation program (MAPEP). The acquisition of the spectrum and its analysis were carried out using Genie 20009 Canberra Software with complementary with packages of Interactive Peak fit, Geometry Composer and Quality Assurance. The minimum detectable activities (MDA) with 95% confidence level of the radioisotopes under investigation are listed in Table 1. The detection of MDA and the detection limit were carried out according to the methods and the instructions of Reguigui (2006). MDA was calculated using the following equations (Reguigui, 2006):

$$MDA = \frac{L_D}{T\ x\ eff\ x\ Br\ x\ m}$$

Where L_D = the detection limit, T = the counting time (sec), eff = efficiency, Br = branching ratio and m = mass.

$$L_D = L_C + K\sigma_D$$

Where Lc = critical level: below which no signal can be detected, σ_D = standard deviation and K = error probability

Heavy mineral detections

Three locations (distances within the profile) were selected from each of the four profiles for heavy mineral investigation: beach samples representing the beach and the swash zone, 100 m distance samples representing the surf zone, and finally, 800 m distance samples that represent the breaker zone. These zones are well defined by Ingle (1966). Samples were sieved with a shaker and the mean grain size values were obtained. 5 g of each dried samples was released into a separating funnel using the dense-liquid technique with bromoform (Specific gravity equal 2.8 g/cm^3). Samples were boiled in 10% hydrochloric acid for two minutes in order to disintegrate the samples. Boiled samples were rinsed with water to remove the hydrochloric acid and dried in an oven in order to separate the fine sand fraction.

The procedure as mentioned by Joshua and Oyebanjo (2009) that the mixture was vigorously stirred and left for about 5 min was observed. The heavy minerals present in the samples with specific gravity > 2.85 g/cm^3 were allowed to settle to the bottom of the separating funnel or after which the filtrate (heavy mineral) were thoroughly washed with acetone to remove any traces of bromoform. The weight percentages of heavy minerals residue (HM%) and the light minerals (LM%) have been calculated. The heavy minerals were mounted on slides with the aid of Canada balsam (Mange et al., 1992). Heavy minerals were identified and counted using polarizing microscope (Carl-Zeiss – West Germany).

Index figure

Ratio of heavy to light minerals calculated as index figure percentage.

Zircon, tourmaline and rutile proportions (ZTR) index

ZTR is the percentages of zircon, tourmaline and rutile in the non-opaque heavy minerals suites. It is to assess the mineralogical maturity of sediments (Garzanti and Andò, 2007). Dill (1995) referred a high ZTR index to a high degree of weathering where the unstable minerals were eliminated by dissolution. The “ZTR” index, which is a quantitative definition of mineral assemblage, was calculated using the following equation:

$$ZTR\%\ Index = \frac{Zircon + Tourmaline + Rutile}{\sum non - opaque}\ x\ 100$$

RESULTS AND DISCUSSION

Depth profile

Normally, it could be found from both status; accretion and erosion at different depths within the same profile (CoRI, 2001) in Nile Delta coast. In order to identify the recent erosion and accretion parts of the four profiles under investigation, matching between data of the survey done during 2001 against the other one on 2002 was carried out. Figure 2 shows the temporal changes of the four profiles; P1 and P2 (west of Rashid) and P3 and P4 (west of El-Burullus). To show the four profiles in one figure, the depth values of each profile subtracted with fixed number per profile (P2 - 2, P3 - 4 and P4 - 6) for the two years data. The first profile (P1) was appeared in Figure 2 as erosion profile except only at 300 m distance at about 3 m depth. While the second profile (P2) was recognized during the sampling time as accretion profile

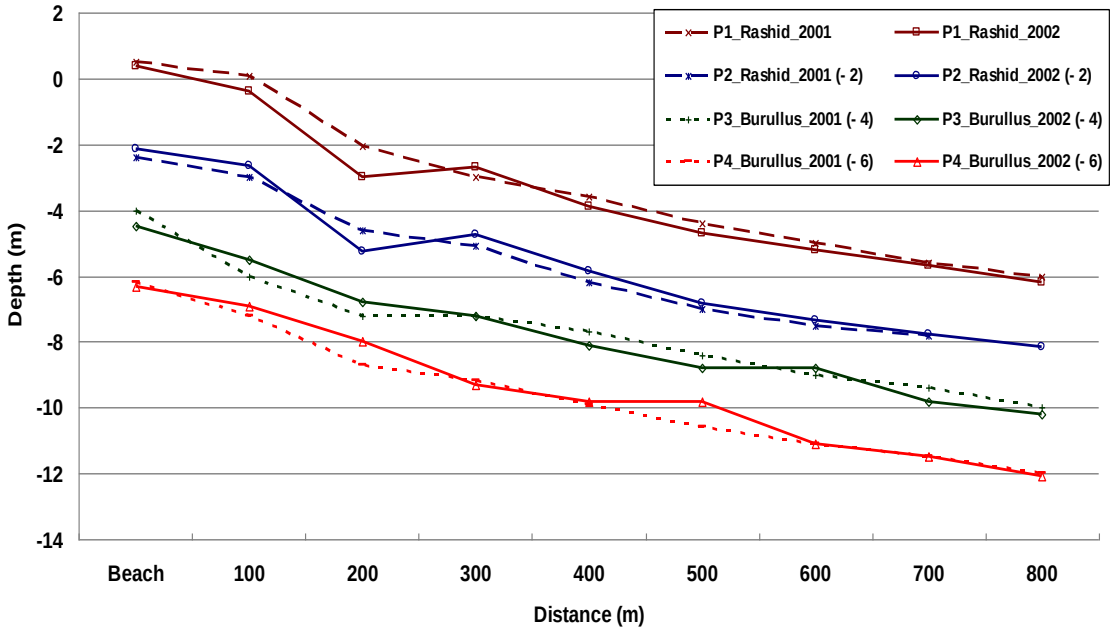

Figure 2. Depth profiles at west of Rashid estuary and El-Burullus outlet during 2001 and 2002.

except at distance 200 m. Longitudinal trough has been observed at Rashid profiles extending parallel to the shore line at 200 m distance from the baseline. Concerning west El-Burullus profiles, fluctuation between erosion and accretion within the same profile has been observed. Measurements indicated that seabed slope was steeper near the shore than at the off shore zones according to the decreasing of the bed grain size. Also, it was noticed that, there are submerged bars parallel to the shoreline. This was confirmed by the finding of El-Kolfat (2005). The beach suffered severe erosion while 100 and 200 m distances sampling point exposed to heavy accretion and it reverse again to erosion and accretion at the rest of the profile of P3. The fourth profile (P4) has heavy accretion situation in many parts, such as at 100, 200 and 500 m distances. The beach of the second profile (P2) was recognized as the only accretion one among the others three erosional beaches. On the other hand, the 100 m distance sampling site at P1 was the only erosional status among the other accretional sites at the same distance.

Mean grain size distribution

The mean grain-size distribution and the sorting of the sediment profiles are presented in Figure 3. The mean grain size of sediments at west El-Burullus beach was found coarser than those in the west of Rashid beach. The detected mean grain sizes of the beach sediments were sorted as 0.239, 0.26, 0.201 and 0.189 mm for P3, P4, P2 and P1, respectively. Reverse distribution was recognized, and sediments grain size at 100 to 400 m distances of P1 were found coarser with lower sorting values than sediments at the same distances of El-Burullus. Moreover, coarser grain size was detected at the second profile (P2) of Rashid, at distances 100 to 200 m less than the distances at El-Burullus. The sediments at distances from 500 to 800 m showed similar trend with a significant decrease of grain size values ranged from 0.069 to 0.097 mm.

Radioactivity distribution

Natural single occurrence (^{40}K) and series (^{238}U and ^{232}Th) radioisotopes were detected in all sediment samples under investigation. The distribution of ^{238}U series members along the four profiles are shown in Figures 4, 5, 6 and 7 and of ^{232}Th series in Figures 8 and 9. The highest averages of ^{226}Ra, ^{214}Pb, ^{214}Bi and ^{210}Pb (as ^{238}U series) were 104.37±84.66, 45.60±37.83, 38.43±32.49 and 35.69±24.86 Bq/kg, respectively and ^{228}Ra and ^{212}Pb (as ^{232}Th series) were 54.26±56.66 and 42.18±44.66 Bq/kg, respectively. These highest averages concentrations have been detected at the third profile (P3) west of El-Burullus outlet. The highest average values of ^{40}K concentration were detected at P2 and P4 (404.49±125.81 and 403.26±20.48 Bq/kg, respectively) ^{137}Cs has been detected at limited number of sites and P4 was found as the relatively higher values compared with the other profiles with average value 0.86 Bq/kg. Generally, in coastal area, the major source of ^{137}Cs is coming from atmospheric deposition (Zhiyong et al., 2010).

The distribution of the detected radionuclides was

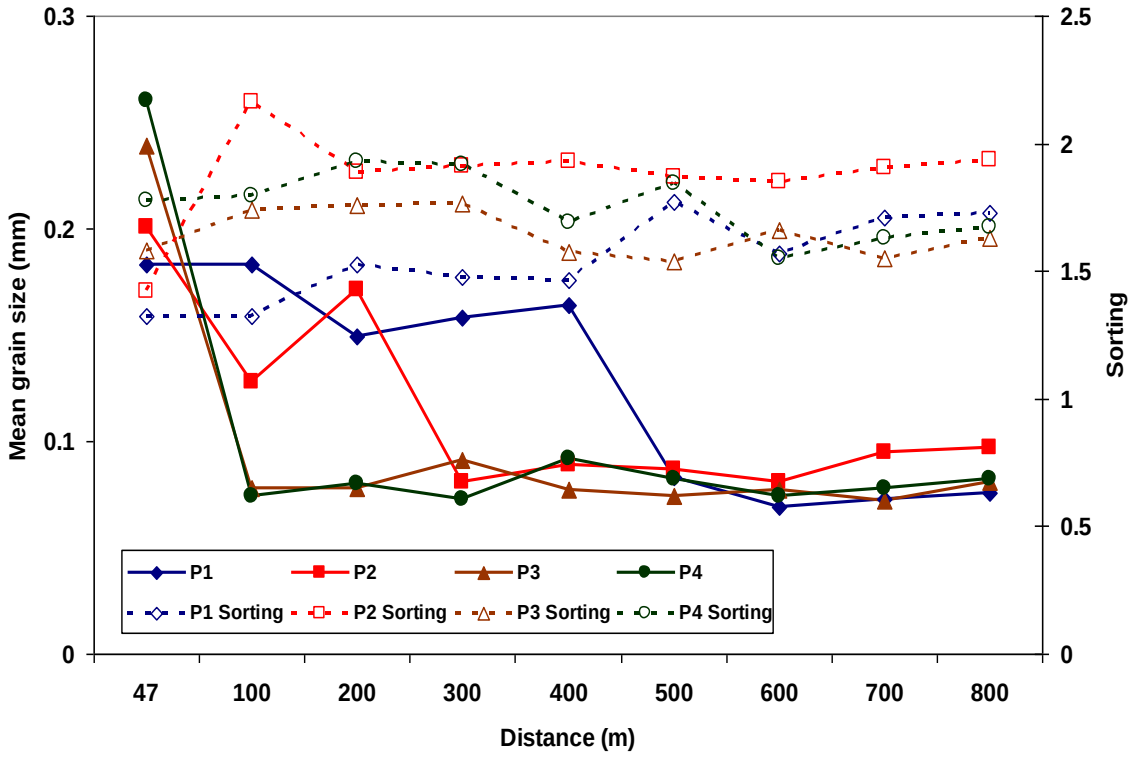

Figure 3. Mean grain size (mm) and sorting (standard deviation) of sediments at P1 to P4 profiles during 2002.

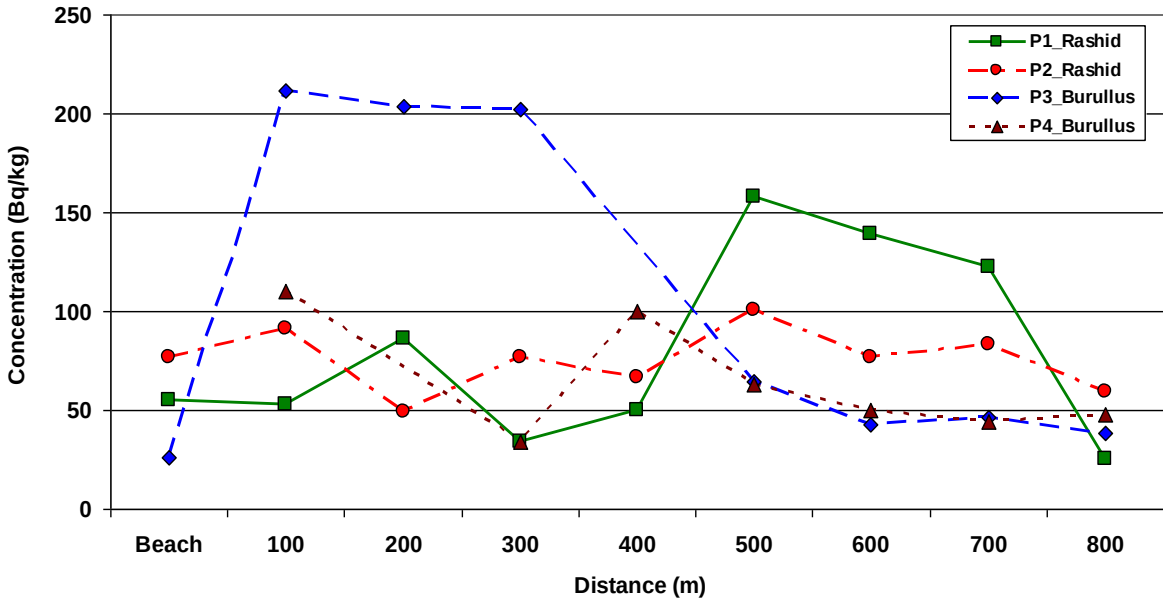

Figure 4. ^{226}Ra concentration (Bq/kg) at Rashid and Burullus coastal sediments profiles during 2002. The highest averages concentrations were detected at the third profile (P3).

varied with depth and distances at each profile as shown in Figures 4, 5, 6, 7, 8, 9 and 10. At the beach, the second profile at Rashid (P2) which is characterized by accretion status, exhibited the highest ^{238}U and ^{232}Th decay series activities, while P3 showed the lowest. Dramatically increase in radioactivity concentration in ^{238}U and ^{232}Th decay series of P3 sediments under its accretion condition was recognized at 100, 200 and 300

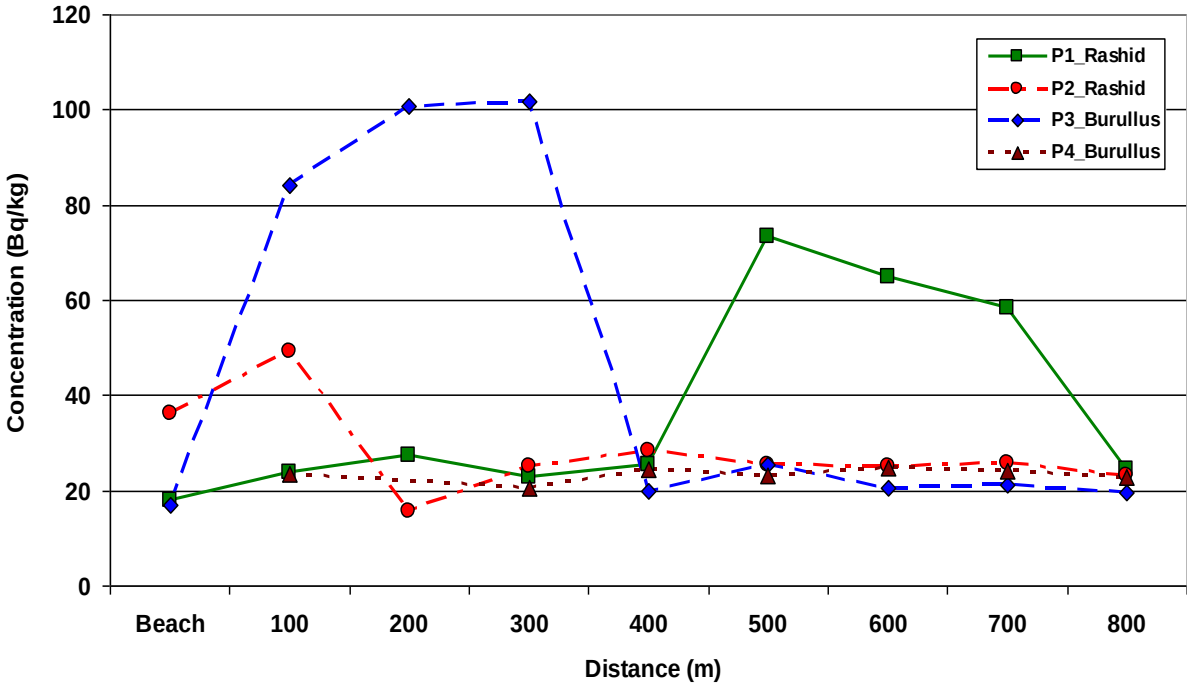

Figure 5. ^{214}Pb concentration (Bq/kg) at Rashid and Burullus coastal sediments profiles during 2002. The highest averages concentrations were detected at the third profile (P3).

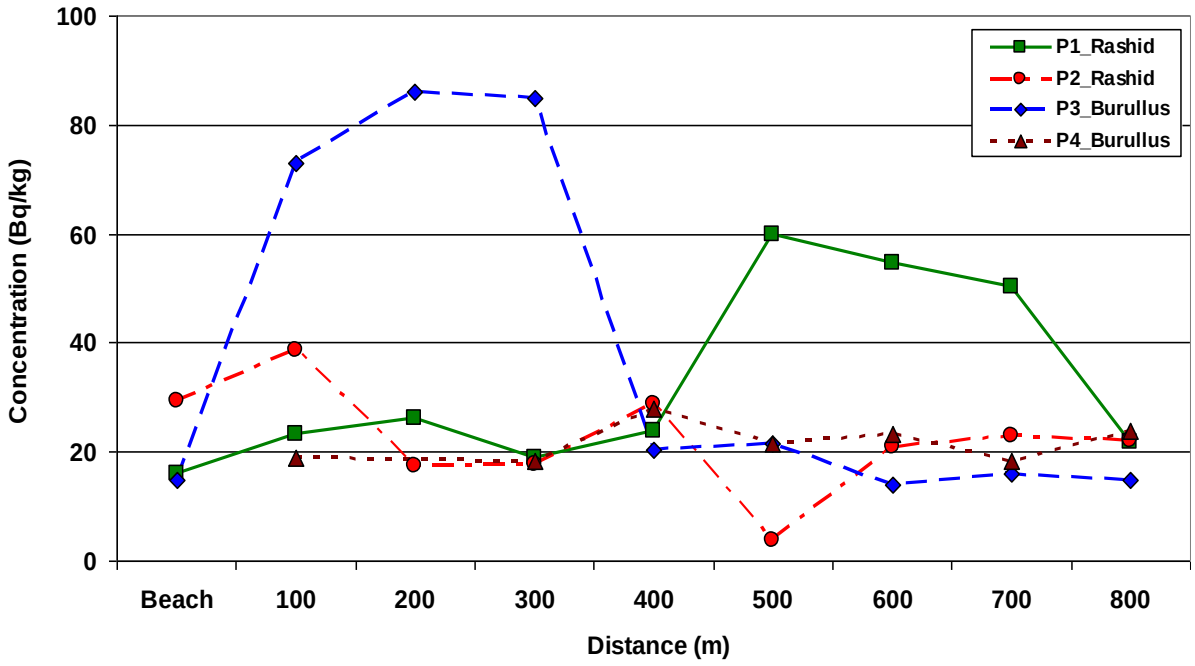

Figure 6. ^{214}Bi concentration (Bq/kg) at Rashid and Burullus coastal sediments profiles during 2002. The highest averages concentrations were detected at the third profile (P3).

m distance samples as shown in Figures 4, 5, 6, 7, 8 and 9. On the other hand, relatively higher concentrations of ^{238}U and ^{232}Th decay series were observed at P1 (Rashid) under its erosion condition at 500 to 700 m distances. This distribution of radioactivity could synchronize with the mean grain size distribution at the same places, which it has finer grains trapped between coarser grains. The relation between radioactivity

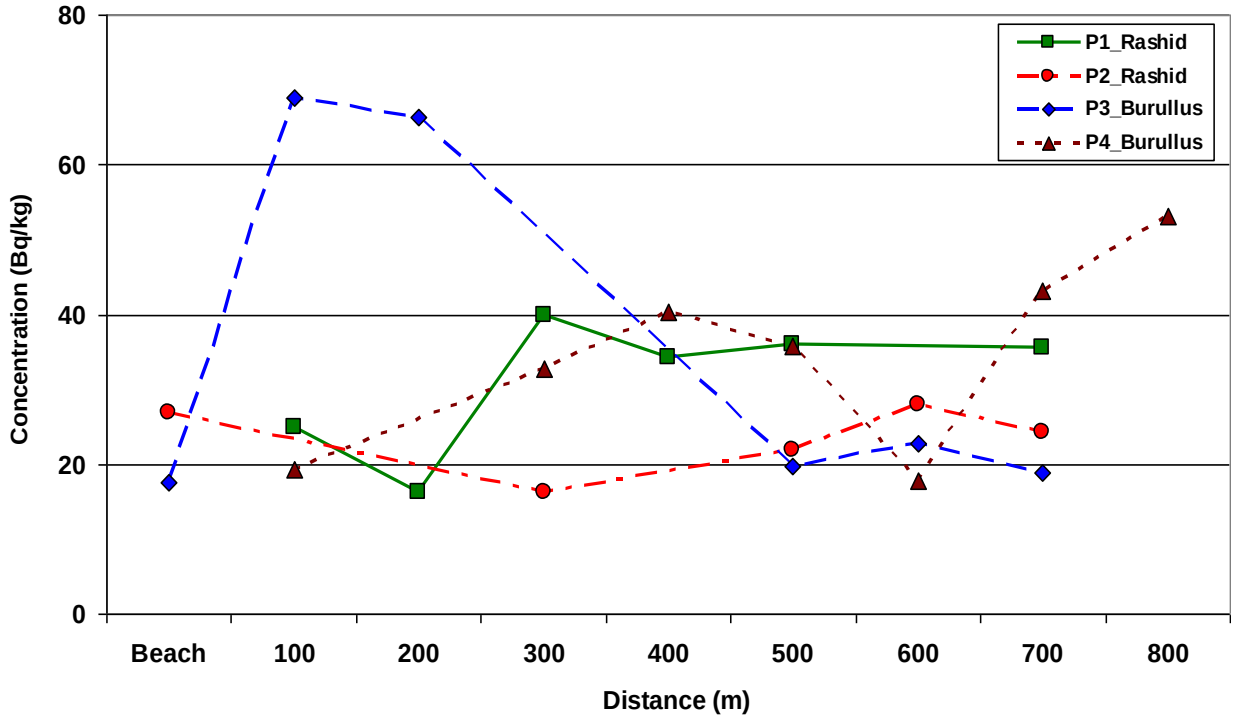

Figure 7. ^{210}Pb concentration (Bq/kg) at Rashid and Burullus coastal sediments profiles during 2002. The highest averages concentrations were detected at the third profile (P3).

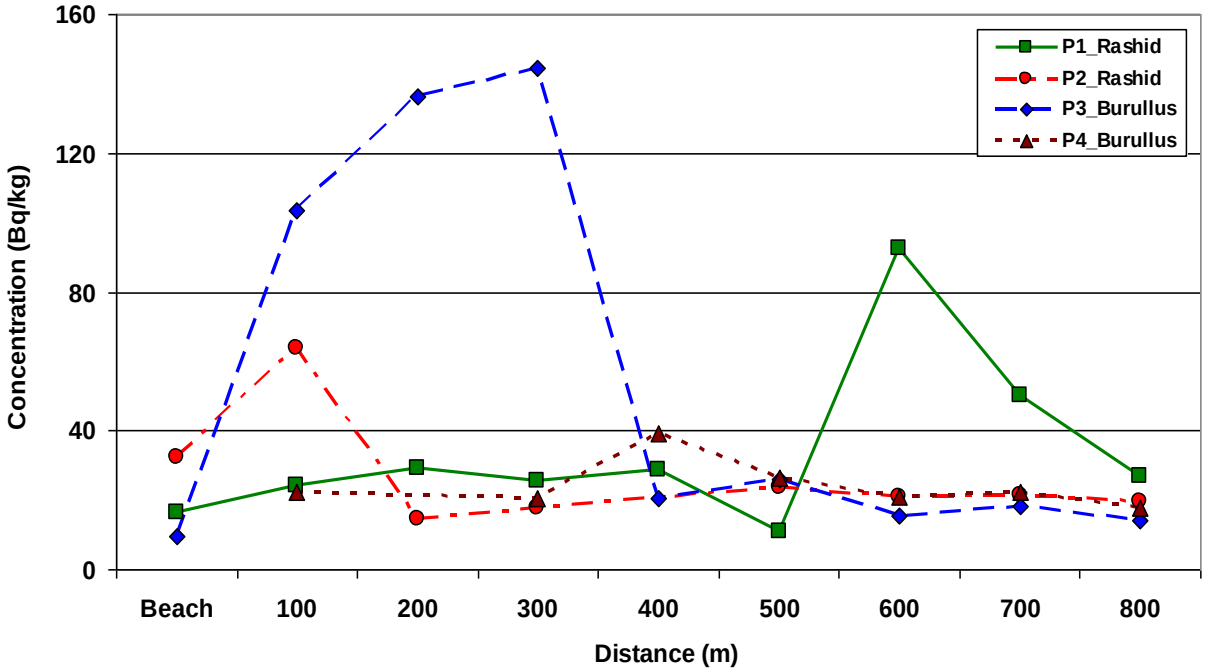

Figure 8. ^{212}Pb concentration (Bq/kg) at Rashid and Burullus coastal sediments profiles during 2002. The highest averages concentrations were detected at the third profile (P3).

distributions with grain size of sediments was confirmed by Vassas et al. (2006). They studied grain size parameters and heavy minerals content in connection with the distribution of U, Th and ^{40}K in a cross-shore

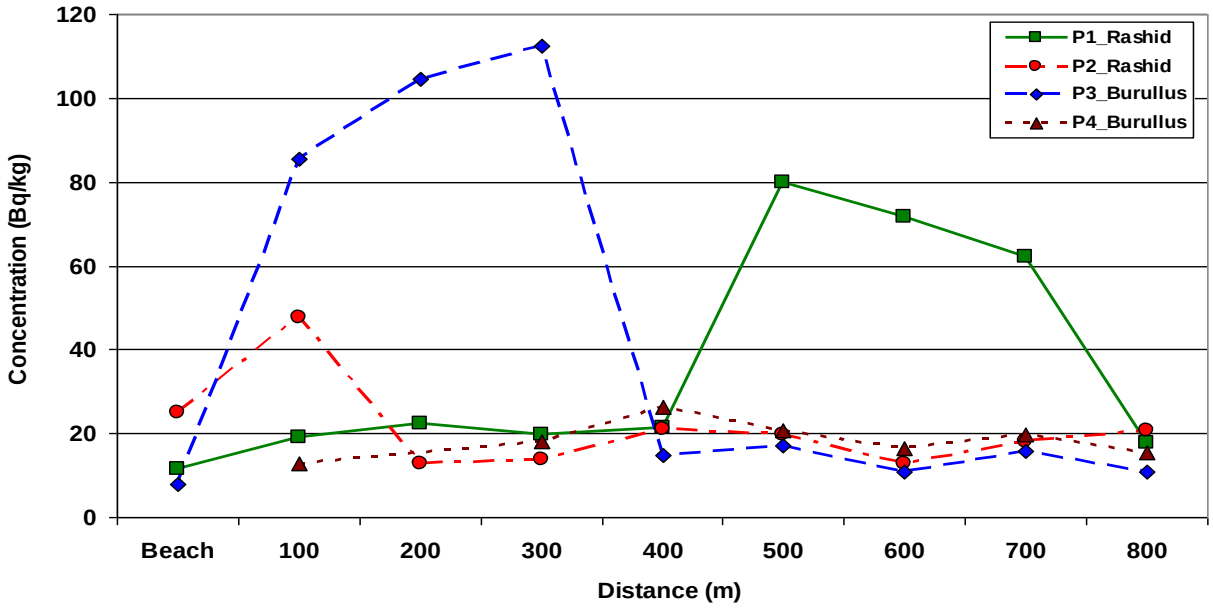

Figure 9. ^{228}Ra concentration (Bq/kg) at Rashid and Burullus coastal sediments profiles during 2002. The highest averages concentrations were detected at the third profile (P3).

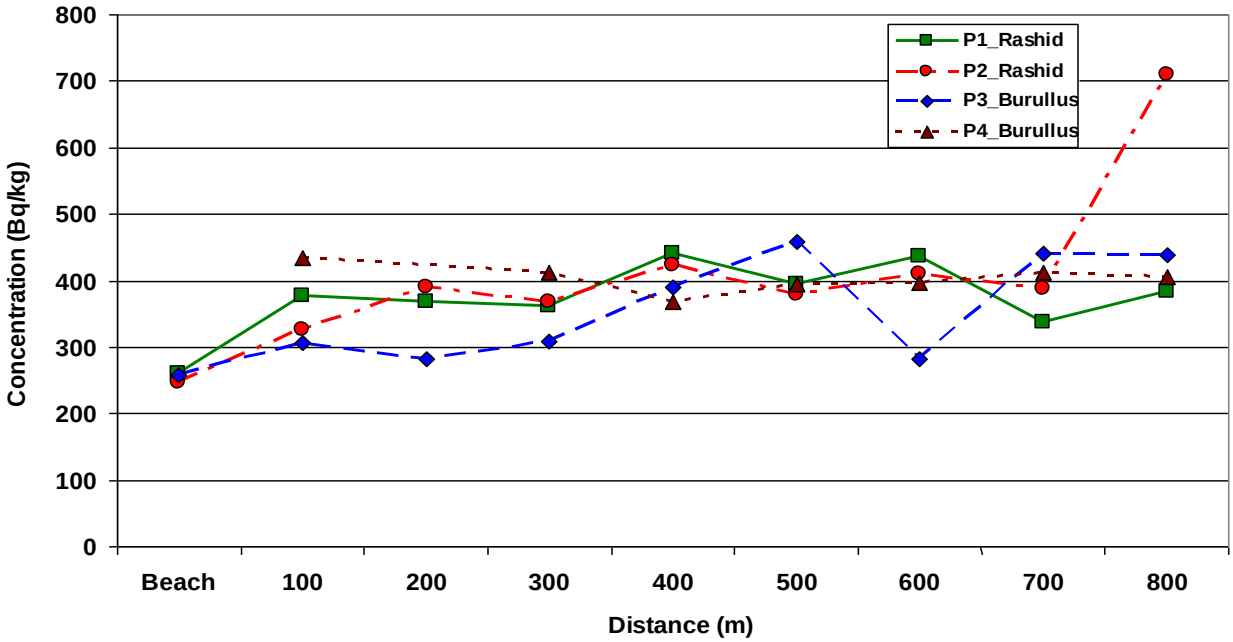

Figure 10. ^{40}K concentration (Bq/kg) at Rashid and Burullus coastal sediments profiles during 2002.

profile and they found that the <0.2 mm fraction contains more than 50% of radioactive elements and heavy minerals (especially zircon). Heavy minerals were the main contributors to high levels of external radiation. Figure 10 illustrate the irregular distribution of ^{40}K at the four profiles. The maximum ^{40}K concentration value (709.10 Bq/kg) was detected at 800 m distance of P2 and minimum value (246.80 Bq/kg) was detected at the beach of P2.

Heavy minerals analysis

Total heavy and light minerals percentages in the profile sediments have been estimated and presented in Table 2

Table 2. Heavy minerals percentages in sediments of the beach, 100 and 800 m distances, along the four profiles situated at the west of Rashid estuary and Burullus outlet.

	Beach				100 (m)				800 (m)			
	P1	P2	P3	P4	P1	P2	P3	P4	P1	P2	P3	P4
HM (%)	4.77	13.79	2.63	0.80	12.76	14.17	38.16	11.75	7.50	22.16	13.72	14.20
LM (%)	95.23	86.21	97.37	99.21	87.24	85.83	61.84	88.25	92.50	77.84	86.28	85.80
IF	0.05	0.16	0.03	0.01	0.15	0.17	0.62	0.13	0.08	0.28	0.16	0.17
ZTR	6.67	17.79	39.32	8.44	1.59	1.87	2.01	5.23	14.67	20.16	0.75	3.35
Heavy minerals												
Opaques	8.00	22.38	22.37	17.20	6.80	23.75	19.07	4.01	23.37	26.70	2.93	18.68
Hornblende	20.00	23.81	14.74	17.74	10.65	15.20	17.44	30.77	15.68	14.49	30.40	31.52
Tremolite + Actinolite	0.00	0.00	0.00	0.00	1.48	0.95	0.00	1.00	0.30	0.00	0.00	0.00
Augite	53.33	33.81	25.26	34.41	31.66	27.79	30.00	32.44	32.84	32.67	23.81	27.63
Epidote	4.00	1.90	0.53	16.13	19.53	18.29	23.26	17.73	3.85	9.09	35.90	12.45
Garnet	0.80	1.43	2.37	0.54	1.48	0.48	0.23	0.00	0.00	0.28	0.73	0.39
Zircon	4.53	11.43	29.47	6.99	0.59	1.19	0.93	4.68	10.06	13.64	0.37	2.33
Rutile	0.27	0.95	0.53	0.00	0.00	0.24	0.70	0.33	0.89	0.85	0.37	0.00
Tourmaline	1.33	1.43	0.53	0.00	0.89	0.00	0.00	0.00	0.30	0.28	0.00	0.39
Apatite	0.00	0.00	0.00	0.54	0.00	0.71	0.00	0.00	0.00	0.28	0.73	0.39
Kyanite	0.80	0.48	0.00	0.00	0.59	0.95	0.00	0.00	1.18	0.28	0.73	0.39
Monazite	0.53	1.43	4.21	1.08	0.30	0.71	0.70	1.00	1.18	0.00	0.37	5.84
Staurolite	0.53	0.95	0.00	1.61	0.00	0.00	0.00	0.00	0.59	0.00	0.00	0.00
Biotite + Chlorite	5.87	0.00	0.00	3.76	26.04	9.74	7.67	8.03	9.76	1.42	3.66	0.00
Total	100	100	100	100	100	100	100	100	100	100	100	100

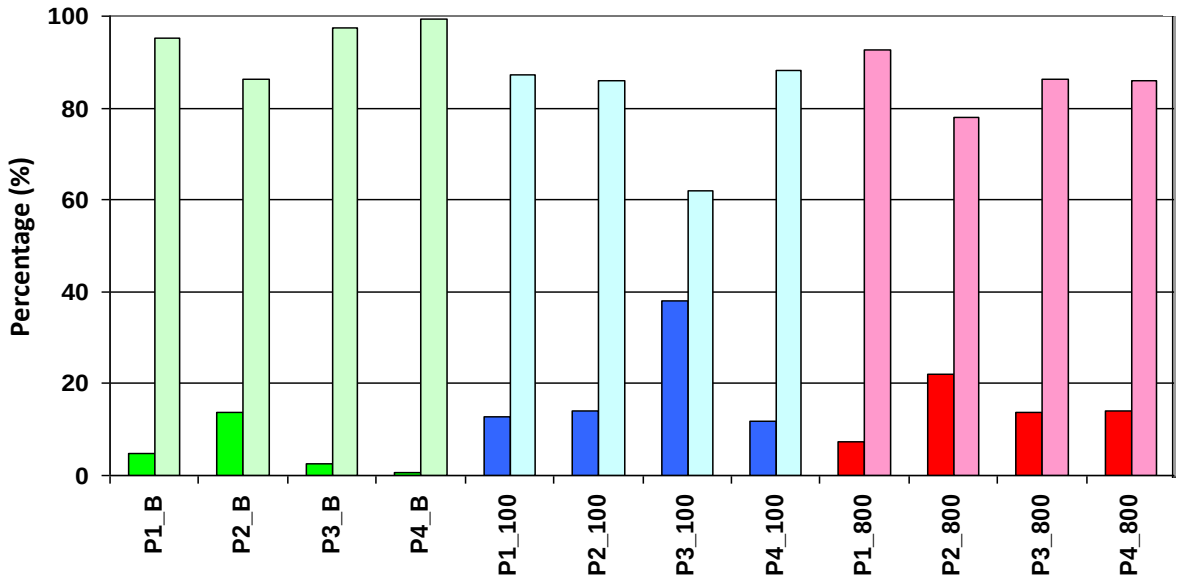

Figure 11. Percentages of heavy minerals (dark color) and light minerals (light color) in coastal sediments at beach, 100 and 800 m distances in four different profiles west of Rashid estuary and Burullus outlet during 2002.

and Figure 11. Index figure (IF) was calculated to recognize the higher percentage of the heavy minerals than the light minerals. Relatively high IF (0.16) was found at beach of P3 compared with the other calculated values of the others beaches under investigation. At 100 m distances, relatively higher IF value (0.62) at P3 which

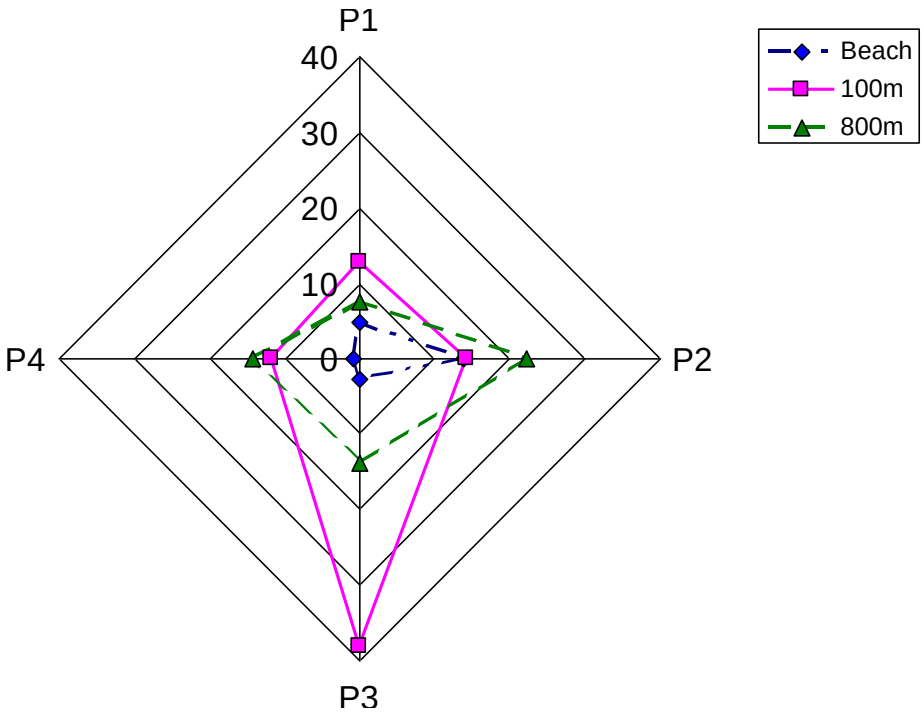

Figure 12. Assembled heavy minerals percents of the four coastal sediment profiles at beach, 100 and 800 m west of Rashid and El-Burullus coastal areas.

indicated the higher percentage of heavy minerals. Both the beach of P2 and at 100 m distance of P3 were characterized by relatively higher ^{238}U and ^{232}Th series compared with the other profiles as shown in Figures 4, 5, 6, 7, 8 and 9. Also, the heavy minerals percentage (38.16%) at 100 m distance of P3 was higher than the beach of P2 (13.79%) and this variation was matched with their radioactive contents variation.

The recorded heavy mineral constituents of the coastal sediments composed of great variety of minerals. Microscopic study revealed that the heavy minerals assemblage consists of opaques, hornblende, tremolite, actinolite, augite, epidote, garnet, zircon, rutile, tourmaline, apatite, kyanite, monazite, staurolite, biotite and chlorite. The percentages of the identified heavy minerals are listed in Table 2. Opaques, hornblende, augite, epidote, biotite and chlorite were the dominant heavy minerals. Also, minor amounts of garnet, zircon, rutile, tourmaline, kyanite and monazite was detected. Tremolite, actinolite, apatite and staurolite were found at scarce amounts at some limited sites along the profiles. The scarcity of these minerals in the sedimentary deposits of the profiles indicated low abundance in the adjacent parent rocks.

Assembled of heavy minerals percents at the beach, 100 and 800 m distances of the four profiles under investigation are plotted together in Figure 12, taking into consideration that three beaches were subject to erosion (P1, P3 and P4) and one (P2) was under accretion condition. The beach site of P3 was subjected to severe erosion where high percentages heavy mineral residues were recorded. Figure 12 illustrated that beaches of the four profiles contain lesser amount of heavy minerals compare to 100 and 800 m distances. Large amount of heavy minerals was found at 100 m distance of the four profiles. This is could be due to the fact that, the 100 m distance acted as the first sink area of the dense and heavy sediment transported from the beach. The highest amount of heavy minerals was observed at 100 m distance of P3 which characterized the highest ^{238}U and ^{232}Th content. The high amount of radioactive materials in this site was mainly attributed to the presence of high amount of radiogenic heavy minerals.

The major contributors to enhance levels of radiation are monazite, and to a lesser extent zircon compared to other minerals (Deer et al., 1997; Mohanty et al., 2004). Significant concentrations of monazite and zircon were found throughout all the profiles. Their distributions at three distances of the four profiles under investigation are presented in Figure 13. Chlorite, biotite, tourmaline and apatite could also play a significant role in uranium and thorium distribution (Dahlkamp, 2009). Rutile showed similar behavior with zircon and tourmaline, for example, strong resistance to weathering and multiple sediment provenances (Mange and Morton, 2007). Rutile displayed only scattered minor concentrations in the study area. Monazite percent at 100 m distance of P3 was recognized as the highest value among the four profiles shown in Figure 13, which demonstrated with the higher values of ^{238}U and ^{232}Th. On the other hand, monazite at the beach sample of P2 showed the highest percentage

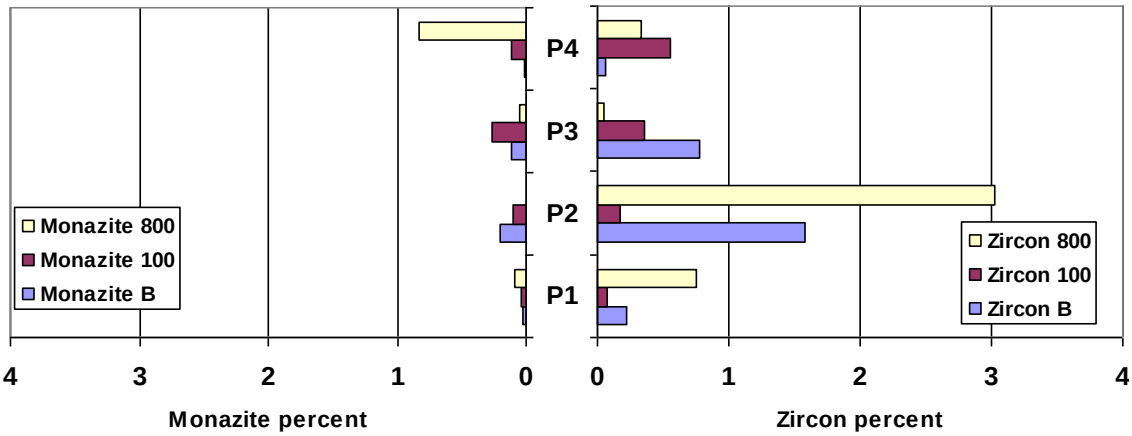

Figure 13. Monazite and zircon percent of heavy minerals detected at beach, 100 and 800 m sediments collected from different profiles at west of Rashid and El-Burullus coasts.

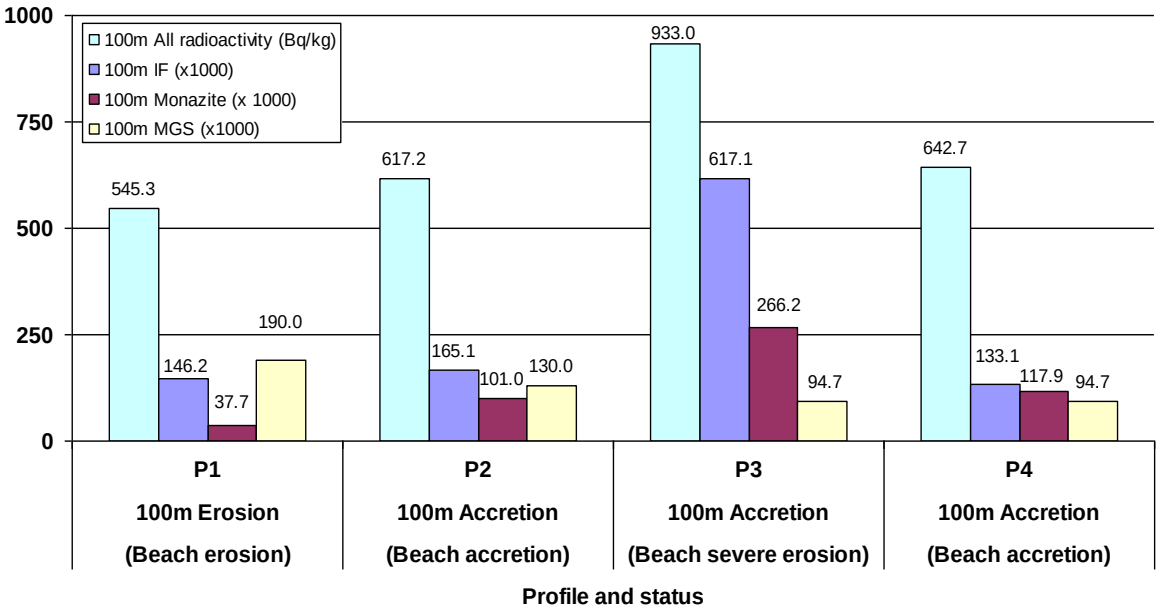

Figure 14. Comparative study of total radioactivity detected (Bq/kg), IF, Monazite percent and mean grain size (mm) in sediments collected at 100 m distance in the four profiles during 2002.

among the beaches and synchronized with the higher values of ^{238}U and ^{232}Th. Conversely, positive correlation (r = 0.7) was observed between the distribution of light minerals percents with the average concentrations of ^{40}K at 100 m distance in the four profiles under investigation. The average concentrations of ^{40}K were 306.5, 326.2, 377.3 and 434.6 Bq/kg, in coincidence with the percentage of the light minerals which are 61.84, 85.83, 87.24, and 88.25% at P3, P2, P1 and P4, respectively.

The higher values of ZTR index, which represented the ultrastable minerals (zircon, rutile and tourmaline) in the superficial sediments, were (39.32, 20.16, 17.79 and 14.67) at the beach of P3, 800 m distance of P2, at the beach of P2 and at 800 m distance of P1, respectively, This relatively high abundance attributed to the provenance. In contrast, the ZTR index values of the other sites, as listed in Table 2, were display relatively low (<10) in these coastal sediments. The highest value of ZTR (39.32) was found at the beach of P3 profile implying severe erosion. The maximum ZTR index of 39.32% obtained shows that the sediments are mineralogical immature.

Figure 14 shows the inter-comparison between the results of activity concentrations of all radioactive nuclides detected at 100 m distance of each profiles, together with heavy minerals percentages demonstrated

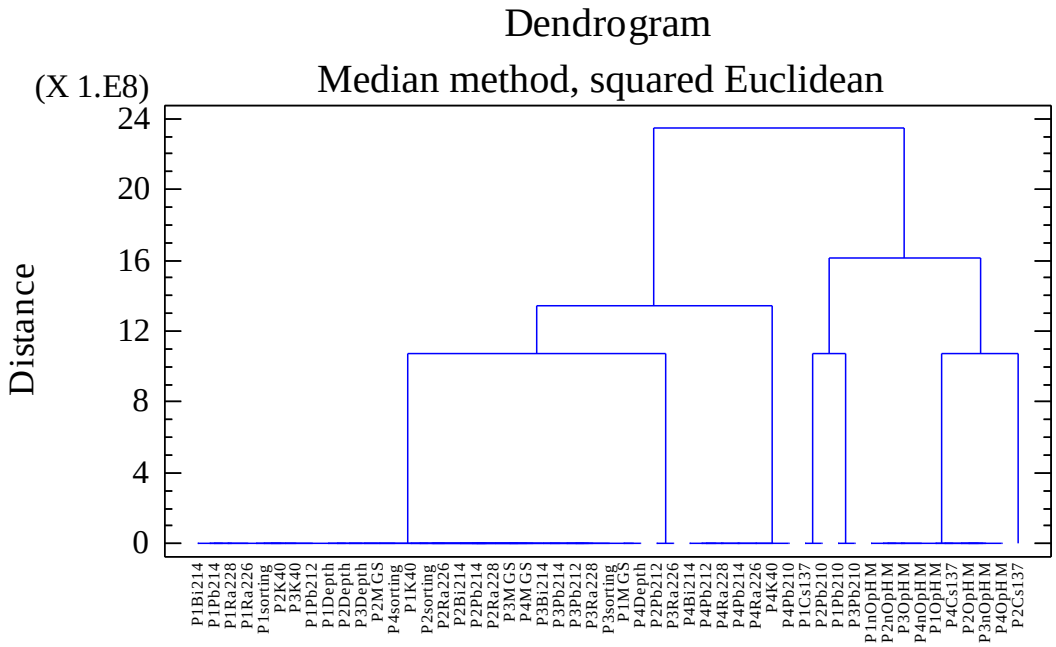

Figure 15. Dendrogram of cluster analysis of all the parameters under investigation. P1 to P4, the four profiles; nOpHM, non-opaque heavy minerals; OpHM, opaque heavy minerals; MGS, mean grain size.

as IF, monazite percentage, mean grain size and erosion and accretion status. The latter three factors multiplied with "1000" in order to show all in one figure. The highest radioactivity values (933 Bq/kg) was determined at 100 m distance of P3 with highest heavy minerals percent (IF = 0.62), highest monazite percent value (0.27%) and lowest mean grain size (0.095 mm). This indicates that there is a strong relationship between the occurrences of radioactive nuclides with the presence of heavy minerals, in particular monazite. Also, this pointed toward importance of the distribution of radiogenic heavy minerals along the coasts. This finding was confirmed by the work of Mohanty et al. (2004) that the highest concentrations of ^{232}Th and ^{238}U were found in monazite compared with the other heavy minerals. Greenfield et al. (1989) confirmed the relation of radiogenic heavy minerals with the transportation of beach sand. Moreover, the grain size distribution plays an important role in this relation. This is in consistent with the finding of Vassas et al. (2006) that across shore profile, the variability in actinides observed at the eastern part of Beauduc spit is mainly explained by variations in heavy and light mineral contents. Such variability can be accounted for by redistribution of the sand caused by erosion/deposition processes occurring in the eastern part of the spit. Severe erosion condition was observed at the beach of P3 and the all accumulated at the next site at 100 m distance which has accretion condition. On the other hand, at P1 the lowest radioactive nuclides (546.3 Bq/kg) are accomplished with low IF, the lowest monazite percent (0.038%) and the highest mean grain size (0.19 mm). Both, the beach and 100 m distance sites at P1 were subjected to erosion condition.

Cluster analysis was performed among all the parameters under investigation using Statgraphics Plus software. Figure 15 shows the dendrogram resulted from the cluster analysis. This procedure has created different clusters from the variables supplied. The clusters are groups of variables with similar characteristics. The first wide cluster is connected with the narrow second at the same distance to gathered all radioactive materials (except ^{210}Pb), mean grain size, depth and sorting values for P1, P2 and P3. Two small clusters are connected at the same distance for the ^{210}Pb of the three profiles P1, P2 and P3. The fourth profile (P4) parameters were clustered as one separate group. Heavy minerals either opaque of non-opaque are gathered together to form one group. ^{137}Cs is disturbed at different clusters. This is because of the large amount of missed data as under the detection limit.

Conclusion

An attempt was made to indicate the relationship between accretion and erosion beaches with the concentrations of different radionuclides and the weight percent of heavy minerals residue of the near shore profile sediments. The distribution of the detected U and Th decay products activities on the beaches of the Nile Delta coast was investigated in order to locate the main areas of enrichment. On the near shore profile, the

variability in U and Th observed at the western side of Rashid and El-Burullus outlets can be mainly explained by the heavy and light minerals contents. Such variability is a consequence of the redistribution of the sand due to coastal processes such as erosion and accretion that take place in the study area or at any place in the world with the same situation. The slope of the profile plays an important role in the concentration of heavy minerals. Furthermore, the study of parameters such as ^{40}K activity, grain size, heavy minerals, monazite and zircon content in the near shore profile provides a better understanding of the concentration processes of radioactivity. At this location, the distribution pattern of the radionuclides along the beach profile is dependent mainly on the sorting of sand grains according to size and density and heavy mineral content (especially monazite). Among the beaches under investigation, relatively higher concentrations of ^{238}U and ^{232}Th decay series members were found at sites that have higher heavy minerals contents, and also, it was detected more in erosional beaches than in accretion ones. Finally, the cross analysis of mineralogical and radiometric data provides a useful tool for a better knowledge of the genesis and characteristics of eroding and accreting beaches.

ACKNOWLEDGEMENTS

The authors would like to thank Prof. Abd El-Moneim Badr, the head of Oceanography Department and the director of Abu Qir Research Station of Coastal Research Institute, National Water Research Center for his efforts and help during the determination of heavy minerals of the sediment samples.

REFERENCES

Alam NM, Chowdury MI, Kamal M, Ghose S, Islam NM, Mustafa MN, Miah MMH, Ansary MM (1999). The 226Ra, 232Th and 40K activities in beach sand minerals and beach soils of Cox's Bazar, Bangladesh. J. Environ. Radioact. 46:243.

Badr AA, Lotfy MF (1999). Tracing beach sand movement using fluorescent quartz along the Nile Delta promontories, Egypt. J. Coast. Res. 15:261-265.

Brai M, Bellia S, Hauser S, Puccio P, Rizzo S, Basile S, Marrale M (2006). Correlation of radioactivity measurements, air kerma rates and geological features of Sicily. Rad. Meas. 41:461-470.

Cascalho J, Fradique C (2007). The source and hydraulic sorting of heavy minerals on the northern Portuguese continental margin. In: Mange M.a. and Wright D.T. eds. Heavy minerals in use, Developments in sedimentology 58:75-110, Elsevier, Amsterdam.

Cochran JK, Krishnaswami S (1980). Radium, thorium, uranium, and 'Pb in deep-sea sediments and sediment pore waters from the North Equatorial Pacific. Am. J. Sci. 280:849-889.

Coelho FDS, Couceiro PRDC, Lopes AL, Fabris JD (2005). Iron oxides and monazite from sands of two beaches in Espirito Santo, Brazil. Quim. Nova 28:233.

Cole KH, Guinasso Jr. NL, Richardson MD, Johnson JW, Schink DR (1986). Uranium and thorium series isotopes in recent sediments of the Venezuela basin, Caribbean Sea. Mar. Geol. 68:167-185.

CoRI (2001). Report on analysis of beach profiles from Rosetta to El-Burullus outlet during the period from April/May to Sept/Oct. 1998, Ministry of Water Resources and Irrigation, National Water Research Center, Coastal Research Institute.

CoRI (2002). Technical report on the monitoring of shore changes of Nile Delta along North Egyptian coast, progress report No. 1 for activity during the period from July to December 2002, Ministry of Water Resources and Irrigation, National Water Research Center, Coastal Research Institute.

Cowell PJ, Stive MJF, Niedoroda AW, Vriend De HJ, Swift DJP, Kaminsky GM, Capobianco M (2003). The coastal tract. Part 1: Aconceptual approach to aggregated modelling of low-order coastal change. J. Coastal Res. 19:812-827.

Dahlkamp FJ (2009). Uranium deposits of the world:Asia, Springer reference, Springer-Verlag Berlin Heidelberg.

De Meijer RJ, Lesscher HME, Schuiling RD, Elburg RD (1990). Estimate of the Heavy Mineral Content in Sand and its Provenance by Radiometric Methods. Nucl. Geophys. 4(4):455-460.

De Meijer RJ, Donoghue JF (1995). Radiometric fingerprinting of sediments on the Dutch, German and Danish coasts. Quat. Int. 26:43-47.

De Meijer RJ (1998). Heavy minerals:from Edelstein to Einstein. J. Geochem. Explor. 62:81.

De Meijer RJ, James IR, Jennings PJ, Koeyers JE (2001). Cluster analysis of radionuclide concentrations in beach sand. Appl. Radiat. Isot. 54:535-542.

Deer WA, Howie RA, Zussman J (1997). Rock-forming minerals:Orthosilicates, Geological Society, London. P. 918.

Dill HG (1995). Heavy mineral response to the progradation of an alluvial fan: Implications concerning unroofing of source area, chemical weathering and palaeorelief (Upper Cretaceous Parkstein fan complex, SE Germany). Sediment. Geol. 95:39-56.

El-Fishawi NM, Badr AA (1991). Mineralogical characteristics of the western Nile Delta coast sediments. Act Mineral.-Petrog. Szeged, XXXII:65-75.

El-Gamal A, Saleh I, Nasr S, Naim M (2004). Radiological assessment of the Egyptian Mediterranean coast, International Conference on Isotopes in Environmental Studies- Aquatic Forum 2004, Monte-Carlo, Monaco 25-29 October 2004, IAEA-CN-118/31P, PP. 396-397.

El-Khatib AM, Denton M, El-sabrouti MA (1993). Isotope identification of Egyptian black sands from Rossetta using neutron activation analysis. J. Fiz. Mal. 14:1-10.

El-Kolfat AI (2005). Coastal characteristics and behaviour for eastern Nile Delta region, Egypt (Burullus- Port Said). Alex. Eng. J. 44(6):899-910.

El-Naggar AM (1990). Environmental radioactivity; Sources and effects on man, Regional. Symp. Environ. Stud. (UNARC), Alexandria University, M. El-Raey (edit).

Frihy OE (2007). The Nile delta:Processes of heavy mineral sorting and depositional patterns, In:Mange M.A. & Wright D.T. eds. Heavy Minerals in use, developments in sedimentology 58, 49-74. Elsevier, Amsterdam.

Frihy OE, Dewidar KM (2003). Patterns of erosion/sedimentation, heavy mineral concentration and grain size to interpret boundaries of littoral sub-cells of the Nile Delta, Egypt. Mar. Geol. 199:27–34.

Frihy OE, Komar PD (1993). Long term shoreline changes and the concentration of heavy minerals in beach sand of the Nile Delta. Egypt. Mar. Geol. 115:253.

Frihy OE, Lotfy MF, Komar PD (1995). Spatial variations in heavy minerals and patterns of sediment sorting along the Nile Delta. Egypt. Sediment. Geol. 97:33.

Garzanti E, Andò S (2007). Plate tectonics and heavy minerals suites of modern sands, In: Mange M.A. and Wright D.T. eds. Heavy minerals in use, Developments in sedimentology Elsevier, Amsterdam. 58:741-763.

Greenfield MB, de Meijer RJ, Put LW, Wiersma J, Donoghue JF (1989). Monitoring beach sand transport by use of radiogenic heavy minerals. Nucl. Geophys. 3:231-244.

Hussein AEM (2011). Successive uranium and thorium adsorption from Egyptian monazite by solvent impregnated foam. J. Radioanal. Nucl. Chem. 289:321-329.

Ingle JC (1966). Developments in sedimentology 5, the movement of beach sand, Elsevier Publishing Company, Amsterdam.

Johanson KJ, Bergström R (1989). Radiocaesium from Chernobyl in

Swedish Moose, Environ. Poll. 61: 249-260.
Joshua EO, Oyebanjo OA (2009). Distribution of Heavy Minerals in Sediments of Osun River Basin Southwestern Nigeria. Res. J. Environ. Earth Sci. 1(2):74-80.
Kaiser MFM, Frihy OE (2009). Validity of the equilibrium beach profiles:Nile Delta Coastal Zone, Egypt. Geomorphology 107:25–31.
Kaiser MFM (2004). Monitoring and modelling the impact of engineering structures on coastline change, Nile Delta, Egypt, Ph.D. Thesis, University of Reading, U.K.
Komar PD (2007). The entrainment transport and sorting of heavy minerals by waves and currents, In Mange, M.A. and Wright, D.T. eds. Heavy minerals in use, developments of sedimentology, 58:3-48. Elsevier, Amsterdam.
Kudrass HR (1987). Sedimentary models to estimate the heavy minerals potential of self sediments, In: Teleki P. G. Dobson M.R. Moore J.R. and Stackelberg U.V. eds. Marine Minerals, D. Reidel Publishing Company, Dordrecht pp. 39-56.
Li WQ, Guinasso Jr NL, Cole KH, Richardson MD, Johnson JW, Schink DE (1985). Radionuclides as indicators of sedimentary processes in abyssal Caribbean sediments. Mar. Geol. 68:187-204.
Mange A, Maria A, Heinz-Maurer FW (1992). Heavy minerals in colour. Chapmam and hall, London, p. 230.
Mange MA, Morton AC (2007). Geochemistry of heavy minerals, In:M.a. Mange and D.T. Wright (Eds.), Heavy minerals in use. Developments in Sedimentology, Elsevier; Amsterdam, 58:345-391.
Miller RL (1976). Role of vortices in surface zone prediction: Sedimentation and wave forces, In:Davis, R.A. Ethington, R.L. (Eds.), Beach and Nearshore Sedimentation. Society of Economic Paleontologists and Mineralogists, Tulsa, Oklahoma. Spec. Publ. 24:92-114.
Mohanty AK, Senguptaa D, Dasb SK, Vijayanc V, Sahab SK (2004). Natural radioactivity in the newly discovered high background radiation area on the eastern coast of Orissa, India. Rad. Meas. 38:153-165.
Nafaa MG (1995). Wave climate along the Nile Delta coast. J. Coast. Res. 11:219-229.
Reguigui N (2006). Gamma Ray Spectrometry, Practical Information. http://www.cnstn.rnrt.tn/afra-ict/NAT/gamma/html/Gamma%20Spec%20V1.pdf.
Saleh I, El-Gamal A, Nasr S, Naim M (2004). Spatial and temporal variations of uranium and thorium series along the Egyptian Mediterranean coast, International Conference on Isotopes in Environmental Studies- Aquatic Forum 2004, Monte-Carlo, Monaco 25-29 October 2004, IAEA-CN-118/113P, PP. 550-551.
Seddeek MK, Badran HM, Sharshar T, Elnimr T (2005). Characteristics, spatial distribution and vertical profile of gamma-ray emitting radionuclides in the coastal environment of North Sinai. J. Environ. Radioact. 84:21.
Smith S, Abdel-Kader A (1988). Coastal erosion along the Egyptian Delta. J. Coast. Res. 4:245-255.
Suman DO, Bacon MP (1989). Variations in Holocene sedimentation in the North American basin determined from 23”Th measurements. Deep-Sea Res. 36:869-878.
USEPA (2011). Radiation protection, about TENORM, U.S. Environmental Protection Agency. http://www.epa.gov/radiation/tenorm/about.html.
Vassas C, Pourcelot L, Vella C, Carpe´na J, Pupin JP, Bouisset P, Guillot L (2006). Mechanisms of enrichment of natural radioactivity along the beaches of the Camargue, France. J. Environ. Radioact. 91:146-159.
Veigaa R, Sanchesa N, Anjosa RM, Macarioa K, Bastosa J, Iguatemya M, Aguiarb JG, Santosb AMA, Mosqueraa B, Carvalhoa C, Baptista Filhoa M, Umisedoc NK (2006). Measurement of natural radioactivity in Brazilian beach sands. Rad. Meas. 41:189-196.
Zhiyong L, Shaoming P, Xuying L, Jianhua G (2010). Distribution of ^{137}Cs and ^{210}Pb in sediments of tidal flats in north Jiangsu Province. J. Geogr. Sci. 20(1):91-108.